Accepted Manuscript

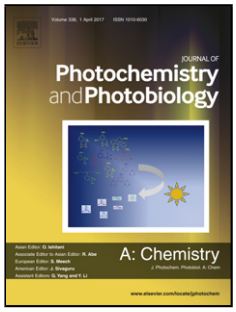

Title: Heterogeneous photo-Fenton process mediated by Sn-substituted goethites with altered OH-surface density

Author: Ana L. Larralde Diego Onna Keyla M. Fuentes Elsa E. Sileo Mirabbos Hojamberdiev Sara Aldabe Bilmes

PII: S1010-6030(19)30300-4
DOI: https://doi.org/doi:10.1016/j.jphotochem.2019.111856
Reference: JPC 111856

To appear in: *Journal of Photochemistry and Photobiology A: Chemistry*

Received date: 20 February 2019
Revised date: 11 April 2019
Accepted date: 10 May 2019

Please cite this article as: Ana L. Larralde, Diego Onna, Keyla M. Fuentes, Elsa E. Sileo, Mirabbos Hojamberdiev, Sara Aldabe Bilmes, Heterogeneous photo-Fenton process mediated by Sn-substituted goethites with altered OH-surface density, *<![CDATA[Journal of Photochemistry & Photobiology, A: Chemistry]]>* (2019), https://doi.org/10.1016/j.jphotochem.2019.111856

This is a PDF file of an unedited manuscript that has been accepted for publication. As a service to our customers we are providing this early version of the manuscript. The manuscript will undergo copyediting, typesetting, and review of the resulting proof before it is published in its final form. Please note that during the production process errors may be discovered which could affect the content, and all legal disclaimers that apply to the journal pertain.

ACCEPTED MANUSCRIPT

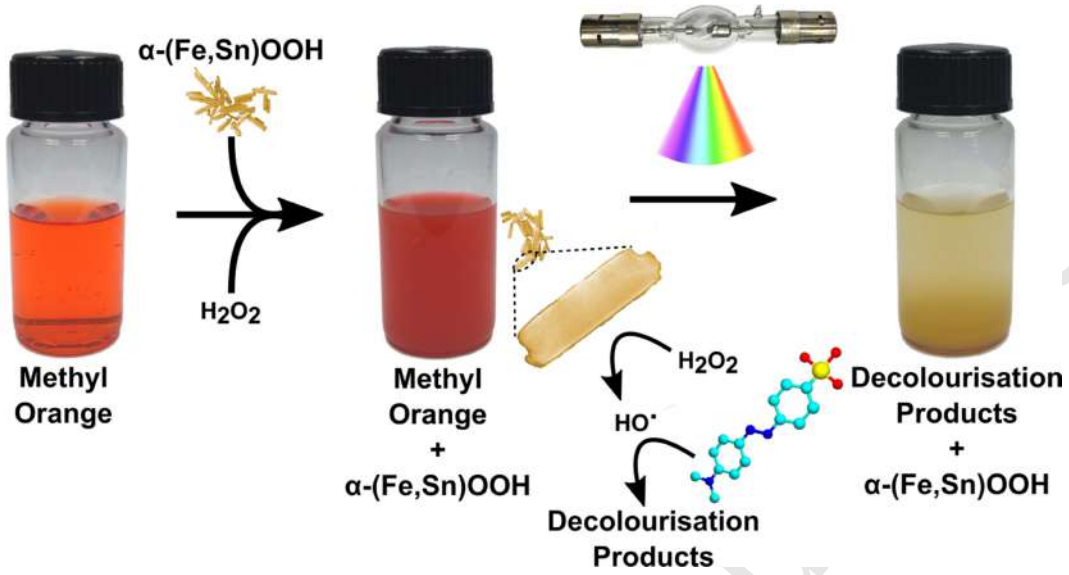

Accepted Manuscript

ACCEPTED MANUSCRIPT

Highlights

- Tin(IV) increases the OH-surface density (OSD) of the goethite.
- Higher OSD leads to greater decolourisation by heterogeneous photo-Fenton.
- Goethite containing 2.1 % Sn(IV) exhibited the greater decolourisation yield (90%).
- Tin participates indirectly in the mechanism of methyl orange decolourisation.

Accepted Manuscript

ACCEPTED MANUSCRIPT

Heterogeneous photo-Fenton process mediated by Sn-substituted goethites with altered OH-surface density

Ana L. Larralde[a,1], Diego Onna[a,b], Keyla M. Flores[a], Elsa E. Sileo[a], Mirabbos Hojamberdiev[c], Sara Aldabe Bilmes[a]

[a] *INQUIMAE, Departamento de Química Inorgánica, Analítica y Química Física, Facultad de Ciencias Exactas y Naturales, Universidad de Buenos Aires. Intendente Güiraldes 2160, Capital Federal (C1428EGA), Buenos Aires, Argentina.*

[b] *Instituto de Nanosistemas, Universidad Nacional de San Martín, 25 de Mayo y Francia, San Martín (1650), Provincia de Buenos Aires, Argentina.*

[c] *Fachgebiet Keramische Werkstoffe/Chair of Advanced Ceramic Materials, Institut für Werkstoffwissenschaften und technologien, Technische Universität Berlin, Hardenbergstraße 40, (10623) Berlin, Germany.*

Abstract

Heterogeneous photo-Fenton process using several pure- and Sn-incorporating goethites was investigated for the decolourisation of methyl orange (MO). The used goethites presented a partial Sn(IV)-for-Fe(III) substitution. Among other properties variations, this partial replacement provoked changes in the OH-surface density (OSD) of the oxo(hydr)oxide. The effect of Sn-for-Fe substitution on the MO decolourisation was investigated by analysing several processes that might occur when combining H_2O_2, UV-Vis irradiation and the iron oxides, with the dye. The best performance was achieved when

Email address: alarralde@qi.fcen.uba.ar (Ana L. Larralde)

Accepted Manuscript

ACCEPTED MANUSCRIPT

a slight substitution of Sn-for-Fe was used, indicating that tin contributes indirectly to the decolourisation by increasing the OSD and assisting the reduction of Fe(III)→Fe(II) through an intermediate between tin and H_2O_2 (SnOOH). The proposed mechanism for the MO decolourisation using the Sn-substituted goethite involves an indirect pathway not previously reported for photo-Fenton process.

Keywords: Substituted goethite, photocatalysis, advanced oxidation processes, reactive oxygen species, dye decolorization, Fenton process

1. Introduction

Wastewater from textile, paper and some other industries is heavily charged with dyes, surfactants and sometimes traces of different metals. These effluents cause damage to the environment, and their treatment is one of the most important matters in water remediation. In the case of dyes, the decolourisation is achieved through adsorption and/or oxidation processes [1, 2]. Among the advanced oxidation processes, the Fenton reaction has been extensively used in the oxidation of a wide range of organic pollutants by means of the *in situ* generation of reactive oxidative species (ROS), such as the hydroxyl radical ($^{\bullet}$OH) [3] (Eq. 1). The degradation of organic pollutants can be accelerated by the combination of Fenton reagents with UV-Vis radiation ($\lambda < 600$ nm). This so-called *photo-Fenton* process gives rise to extra ROS due to the formation of $^{\bullet}$OH radicals by two additional reactions: (i) photoreduction of Fe(III) to Fe(II) (Eq. 2) and (ii) peroxide photolysis (Eq. 3) [4]:

ACCEPTED MANUSCRIPT

$$Fe^{+2} + H_2O_2 \rightarrow Fe^{+3} + {}^{-}OH + {}^{\bullet}OH \quad (1)$$

$$Fe(OH)^{+2} + h\nu \rightarrow Fe^{+2} + {}^{\bullet}OH \qquad \lambda < 580\ nm \quad (2)$$

$$H_2O_2 + h\nu \rightarrow 2\ {}^{\bullet}OH \qquad \lambda < 310\ nm \quad (3)$$

The Fenton process is based on the catalytic reaction between Fe(II) and H_2O_2 in acidic conditions (typically at pH = 3). The recovery and reuse of iron compounds in aqueous media is not simple as Fe species remain soluble; therefore, heterogeneous photo-Fenton arises to overcome this issue. Hence, the search for new sources of stable iron materials has driven the scientific community to investigate efficient heterogeneous solid photo-catalysts, both natural and/or synthetic [5–7]. These materials should exhibit two main features: (i) potential for generating high amount of ROS to boost the photo-Fenton reaction and (ii) stability of the superficial iron species to favour the recovery of the catalysts and posterior reuse [3, 8].

A suitable iron catalyst is goethite (α-FeOOH), which is thermodynamically one of the most stable iron oxides at ambient temperature [9]. Goethite in nature is rarely stoichiometric (OH^-/O^{2-} ratio < 1) and usually contains traces of foreign elements [10]. Similar goethites can be synthetized and the degree of incorporation is influenced by the preparation method [11, 12]. The metal substitution provokes changes not only in its crystallite size, specific surface area (SSA) and surface reactivity; but also in the adsorption of molecules and ions. Furthermore, optical, electrical and photo-catalytic properties of synthetic α-FeOOH can be tuned upon the inclusion of metal cations into their crystal lattice. Over the past years many researchers have

Accepted Manuscript

ACCEPTED MANUSCRIPT

investigated the properties of substituted goethites because of their importance in industrial applications and their role in natural processes [13–18].

Even though goethites have been effectively tested for heterogeneous Fenton and photo-Fenton processes [19–21], substituted goethites have been less explored [22]. The process has been enhanced by the substitution of some transition metals-for-Fe(III). In the case of Cu(II), the enhancement has been attributed to the participation of the thermodynamically favourable redox pairs, Fe^{3+}/Fe^{2+} and Cu^{+}/Cu^{2+}, in the H_2O_2 decomposition cycle [23]. In contrast, the enhancement of the degradation of the organic pollutants found when Fe(III) is substituted by elements that do not form a redox pair, as in the case of Si, the photo-Fenton process is favoured by the electron-hole pairs (e^{-}/h^{+}) generated on the semiconductor surface (Si-FeOOH) under UV light [24].

Among the many reports on the synthesis of substituted FeOOH, information on tin-goethites is still scant [25–27]. Larralde *et al.* [26] have obtained crystalline Sn-containing goethites using milder conditions and a more inexpensive synthetic method. The prepared samples allowed a maximum Sn substitution of 5.5% mol mol^{-1} (expressed as μSn[mol mol^{-1}]=100×[Sn]/([Sn]+[Fe]), [Metal]: mol L^{-1}), and all attempts to synthesise goethites with higher tin content rendered amorphous materials. The Sn incorporation changed the stoichiometry of OH groups and reduced the dissolution rate of goethite in acidic media [25]. On the other hand, it is known that tin forms an intermediate with the H_2O_2 [28] which is used in oxidation reactions of organic compounds. These features could enhance the decolourisation of dyes. To

ACCEPTED MANUSCRIPT

our knowledge, there are no reports of decolourisation of organic matter using Sn-substituted goethites. For the aforementioned, the α-(Fe,Sn)OOH is a potential candidate for its use as a catalyst in the Fenton and photo-Fenton processes.

In this work, pure- and Sn-goethites were investigated as novel heterogeneous photo-Fenton catalysts. A mechanism for methyl orange (MO) decolourisation was proposed through the analysis of the contribution of the semiconductor photo-catalysis (catalyst + UV-Vis light) and heterogeneous Fenton (catalyst + H_2O_2) to the process. These results lead to the development of novel and better photo-catalysts for dyes decolourisation by tuning those properties that can boost the photo-Fenton performance of iron oxides.

2. Experimental section

2.1. Photo-catalyst synthesis and characterisation

Three samples of pure- and Sn-substituted goethites (α-FeOOH) with an effective Sn-content of 0.0, 2.1 and 5.5% mol mol^{-1} were synthesised and fully characterised elsewhere [26]. The guidelines for the preparation of the solids are schematised in Fig. 1. Reagent grade chemicals and high-purity 18 MΩ cm^{-1} water were used for all the syntheses and experiments. The samples were named after their tin effective content as GSn0, GSn2.1 and GSn5.5.

Samples were fully characterised by X-ray diffraction (XRD), Mössbauer spectroscopy, specific surface area (SSA, BET method), point of zero charge

ACCEPTED MANUSCRIPT

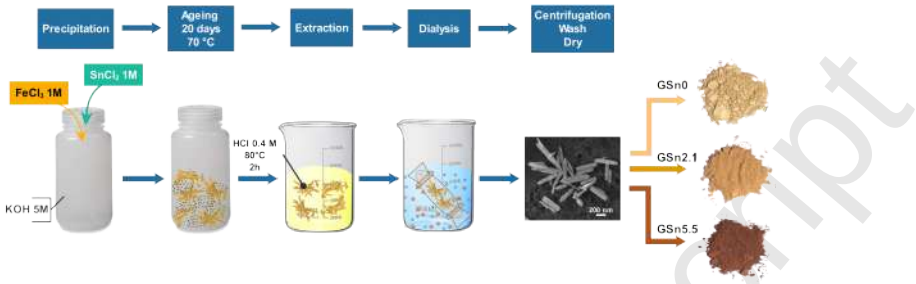

Figure 1: Scheme of the synthesis, extraction and dialysis of the goethites prepared in the presence of Sn(II).

(PZC), thermogravimetric analysis (TGA) and scanning electron microscopy (SEM) in previous works [25, 26].

Reflectance spectra were measured with a SD2000 Miniature Fiber Optic Spectrometer detector from Ocean Optics, using a tungsten halogen light source (HL-2000-LL Mercury Argon Calibration Source) and an ISP-50-8-R-GT integrating sphere.

2.2. Methyl orange decolourisation experiments

MO decolourisation experiments were performed for 60 minutes on stirred solutions at room temperature (*i.e.* 25 °C, 350 rpm) contained in quartz cells. The catalyst (*c.a.* 0.5 g L^{-1}) was dispersed in acidic water (pH = 3, adjusted with $HClO_4$) using an ultrasonic bath of 40 kHz. After sonication, an aliquot of MO was added to reach 0.1 mM concentration. For the experiments performed in the presence of H_2O_2, the molar ratio MO:H_2O_2 was fixed to 1:50. In all cases, the evolution of the reaction as a function of time was monitored by recording the UV-Vis spectra of the remaining MO using an Ocean Op-

ACCEPTED MANUSCRIPT

tics modular spectrometer. For the experiments involving a solid catalyst, an afterwards centrifugation step of 11,000 rpm for 3 min was necessary to recover the solids.

In order to evaluate the contribution of parallel processes to the MO decolourisation, several blank tests (all at pH = 3, 25 °C, 350 rpm) were conducted under different combinations: the direct oxidation was explored by mixing MO and H_2O_2 in the absence of the solid catalysts. Adsorption of the MO onto each of the catalysts was also evaluated in the absence of H_2O_2 after stirring at 350 rpm in darkness. The heterogeneous Fenton process was studied by adding MO and H_2O_2 to a catalyst dispersion in acidic water under the aforementioned conditions. During the photocatalytic and photo-Fenton processes, a Xe lamp of 150 W (AMKO 1000 series) provided with a $CuSO_4$ solution as a IR filter was placed 52 cm in front of the reaction cell. The power of the lamp, determined at the reaction cell distance, was 15.4 mW cm^{-2} ($\lambda_{max} = 520$ nm). Aliquots were taken every 5 min during the first 30 min of reaction and every 10 min for t > 30 min. MO photolysis (with neither H_2O_2 nor catalyst) was also tested using the same conditions. The contribution of pure tin was evaluated using $SnCl_4$ and SnO_2 as catalysts in photocatalysis and heterogeneous photo-Fenton.

For the purpose of confirming the nature of the reactive species taking place in the photo-Fenton process, an aliquot a radical scavenger, tert-butyl alcohol (TBA), was added to the suspended GSn2.1 catalyst along with the MO aliquot. Two sets of measurements were conducted using 25 mM and 50 mM of TBA.

ACCEPTED MANUSCRIPT

3. Results

3.1. Characterisation

The XRD diffractograms and principal peaks indexations for all samples (Fig. S1 (a)) coincide with the reference pattern for the goethite structure and show no evidence of the presence of amorphous ferric oxides (AFO). The Rietveld refinements indicated that Sn was incorporated into the structure by an isostructural replacement of Fe(III) for Sn(IV) as the cell parameters and crystallite sizes increase along with the incorporation (Table S1). Both Fe and Sn oxidation states were determined by Mössbauer spectroscopy and discussed in a previous work [26]. The reported analysis indicated that Sn was incorporated as Sn(IV) and that neither Fe(II) nor Sn(II) were detected.

BET analysis of the N_2 adsorption-desorption isotherms shown in Fig. S1(b) indicated that all the samples presented a low SSA: 26 $m^2\ g^{-1}$ for GSn0, 17 $m^2\ g^{-1}$ for GSn2.1 and 55 $m^2\ g^{-1}$ for GSn5.5 [25]. These results are expected as Cornell and Schwertmann [9] reported that goethites might exhibit SSA ranging from 1 to 200 $m^2\ g^{-1}$ depending on the synthesis method. Moreover, the AFO extraction step could lead to lower SSA values when compared to those samples with no further purification.

The calculated stoichiometry of the OH groups represented in Fig. 2 (a) was determined through TGA analysis (Fig. S1 (c)). The density of surface OH (OSD), showed in Fig. 2 (b) was estimated as the OH/SSA ratio. The hydroxyl groups on the goethite surface can uptake and release protons, resulting in the generation of surface charge due to proton transfer

ACCEPTED MANUSCRIPT

reactions.

Values of the point of zero charge (PZC) (Fig. S1 (d)), defined as the pH at which the electrical charge density on the surface of the particles is zero (illustrated in Fig. 2 (c)), indicate that a slight incorporation of Sn (*i.e.* 2.1%) changed the surface of goethites leading to an increase in the PZC values. Nevertheless, a greater metal incorporation diminished the pH at which the charge density is zero (*i.e.* 4.3 for GSn5.5). This result is in line with the OSD estimation (Fig. 2 (b)) which indicated that a small incorporation of tin firstly increases the OSD values but a larger Sn content decreases it. The incorporation of tin into the structure changed the reactivity and the density of OH^- groups on the surface.

Pure and Sn-substituted samples showed a typical needle shaped morphology (Figs. S2 (a), (b) and (c)) [26]. Length sizes distributions were affected by the tin incorporation, decreasing as the Sn incorporation increased, while width sizes distributions remained almost unchanged (Fig. S2 (d)-(i)). Therefore, pure goethite exhibited the longest particles sizes (507 nm), followed by GSn2.1 (444 nm) and finally GSn5.5 which rendered the shortest particles (308 nm).

The absorption bands position of the iron oxides are generally influenced by the substitution of Fe by other cations [9]. Fig. 3 (a) shows a shift in the position of the absorption bands as tin incorporation increases. The one located at $\lambda \sim 480$ nm moves towards higher wavelengths (red region) while the band at $\lambda \sim 668$ nm shifts to lower values of λ. This result is evinced by the different colours of the solids for the different tin contents

ACCEPTED MANUSCRIPT

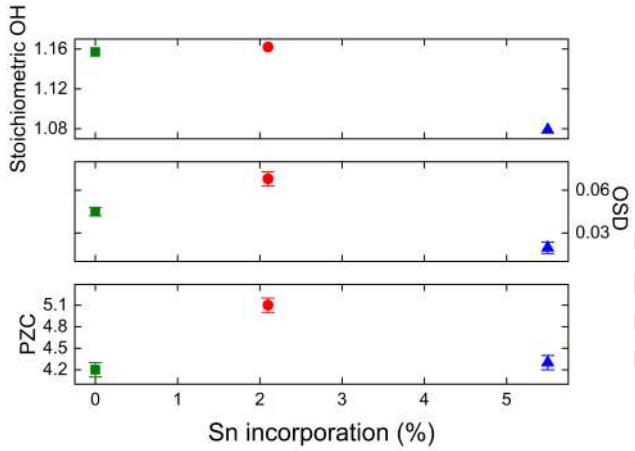

Figure 2: (a) Stoichiometric OH, (b) OH-superficial density (OSD) and (c) PZC values for the pure and substituted samples.

(Fig. 3 (b)). Sample GSn5.5, with an absorption band closer to red, exhibits a brownish colour while the pure sample is ochre. In addition, the spectra indicate that the band gap (E_g) of the samples decreases as Sn substitution increases (E_g = 2.15 eV for GSn0, 2.10 eV for GSn2.1 and 1.84 eV for GSn5.5). This reduction in E_g is consistent with theoretical results reported for Sn substituted hematites [29].

3.2. Methyl orange decolourisation

Decolourisation yields of MO, indicated by a decrease in the absorbance band at λ_{max} = 500 nm (Fig. 4), were determined at pH = 3 in the presence of H_2O_2 and irradiation. The spectra show that a small incorporation of tin enhances the catalytic properties of the goethites, being GSn2.1 the most effective material for decolourisation resulting in a 90% yield in 60 min. Sample GSn5.5 also showed an improvement when compared to the pure

ACCEPTED MANUSCRIPT

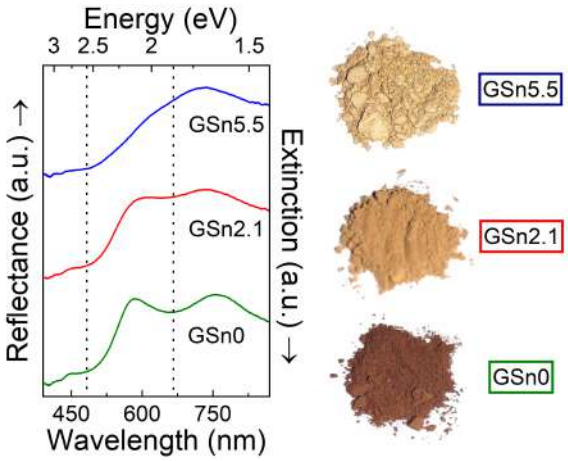

Figure 3: (a) UV-Vis diffuse reflectance spectra of the prepared samples. The arrows in the Y-axis indicate the direction in which the reflectance and the extinction increases. Dotted lines show the position of the absorption bands. (b) Photographs of the goethites powders

sample exhibiting a yield of 36% whereas sample GSn0 only produced a 27% yield.

Several reactions may occur in parallel during the decolourisation of MO via photo-Fenton due to the components of the process (e.g. iron oxide, UV-Vis light, H_2O_2). These reactions could be either in homogeneous phase (photolysis, direct oxidation by H_2O_2 and homogeneous Fenton) or in heterogeneous phase (adsorption, photocatalysis, heterogeneous Fenton and heterogeneous photo-Fenton). For this reason, separate experiments were conducted in order to evaluate the contribution of each process. Given that homogeneous reactions and adsorption were not suitable to explain the decolourisation observed in Fig. 4 (Fig. S3); the main contribution was attributed to the interaction of the catalyst with light and/or H_2O_2 (heterogeneous

ACCEPTED MANUSCRIPT

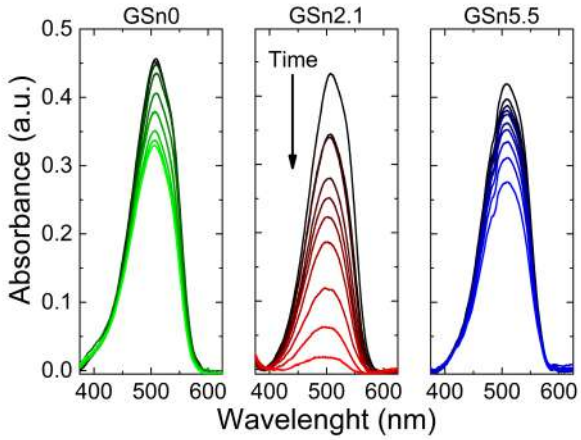

Figure 4: UV-visible spectral changes of methyl orange (MO) during the decolourisation process as a function of reaction time (C_0 = 0.1 mmol L^{-1} of MO, 50 mmol L^{-1} of H_2O_2, 0.5 g L^{-1} of Sn-goethite, pH 3.0, T = 25 °C).

processes). MO decolourisation by means of semiconductor photocatalysis, heterogeneous Fenton and heterogeneous photo-Fenton is shown in Fig. 5.

Changes in the relative absorbance of MO, depicted in Fig. 5 as black triangles, represent the decolourisation by photocatalysis, which is approximately 10% for all samples after 60 minutes. Even though the tin incorporation increases the light absorption of goethite in the visible region (Fig. 4), no significant increment in the decolourisation is observed, suggesting that the Sn-for-Fe substitution does not affect the charge transfer.

However, samples containing Sn show a significant difference when compared to the pure goethite both in Fenton (orange circles in Fig. 5) and photo-Fenton processes (purple squares in Fig. 5). Heterogeneous Fenton experiments (*i.e.* in absence of light) reveal the effect of Sn substitution.

ACCEPTED MANUSCRIPT

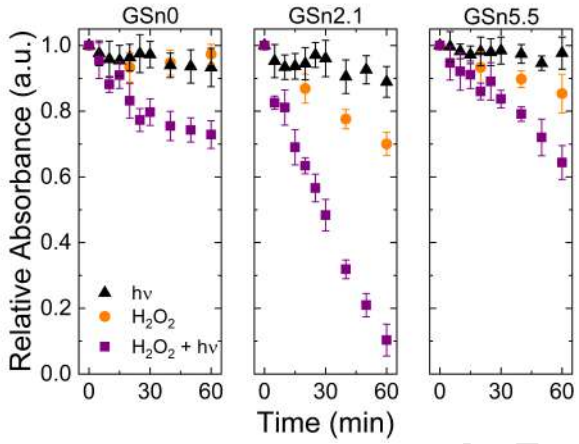

Figure 5: Relative absorbance (at $\lambda_{max} = 500$ nm) of MO in the presence of the catalysts under (▲) photo-catalysis (UV-light), (●) Fenton (H_2O_2) and (■) photo-Fenton (H_2O_2 in the presence of UV-light).

The resulting decolourisation yields were 30%, 16% and 5% for the GSn2.1, GSn5.5 and GSn0, respectively. GSn0 exhibits a low MO decolourisation when compared to published reports [21, 30], probably due to the acidic extraction step of AFO, not usually found in literature. This procedure lowers the PZC value and increases the overall material crystallinity, diminishing the decolourisation rate since amorphous iron materials present higher Fenton efficiency than the crystalline ones [31]. Heterogeneous Fenton results correlate with the tendency observed in Fig. 2 (b), suggesting that the amount of OSD influence the efficiency of the solids. Even though GSn0 and GSn5.5 show similar characteristics regarding the OSD and PZC values, the higher decolourisation obtained with GSn5.5 indicates that the incorporation of tin into the structure does provoke an improvement on the goethite performance.

The noticeable increase in the decolourisation yield for all the samples by

ACCEPTED MANUSCRIPT

combination of irradiation and H_2O_2 (represented by purple squares in Fig. 5), highlights the changes observed in MO spectra in Fig. 4, demonstrating the advantages of the heterogeneous photo-Fenton process mediated by Sn-goethites. In addition, blank tests indicated that pure Sn compounds such as $SnCl_4$ and SnO_2 do no produce degradation (Fig. (S4)). The degradation results with irradiation and H_2O_2 indicate that there is a correlation with the amount of OSD, confirming that the superficial species involved in the photo-Fenton reaction are the same than those of the heterogeneous Fenton process. These results also suggest that the role of the illumination might be to promote the formation of the aforementioned reactive species.

4. Discussion

It is widely accepted that the superficial structure of goethite changes with the incorporation of small amounts of several metal ions [32, 33]. Changes in the structure related to the OSD depends on the metal ion and its amount and, it strongly affects the surface reactivity of α-FeOOH [34]. In the case of Sn, we demonstrated that for the sample GSn2.1, the OSD is higher than for both GSn0 and GSn5.5. This slight substitution of Sn-for-Fe noticeably modifies the catalytic properties of the goethites towards a better decolourisation of the contaminant but a higher incorporation is less effective. A similar trend has been reported for the decolourisation of several dyes under UV-Vis light using Sn substituted hematites, where the maximum decolourisation was obtained at an intermediate Sn content [35].

The photocatalytic reactions are a consequence of the semiconductor na-

ACCEPTED MANUSCRIPT

ture of the iron oxides. This may occur through a direct route (direct hole transfer) and/or an indirect way (ROS formation) [36]. The direct hole transfer is not possible since the adsorption of dye molecules was not detected in these solids (this also disregards the sensitisation effect) [37]. Moreover, the ROS production from the photogenerated charges (reacting with O_2 or H_2O) is not efficient for these materials. These observations account for the obtained results in the photocatalytic experiment, which are in line with those reported by Jelle *et al.*, where α-FeOOH photo-degradated methylene blue with a 40% yield in 5 hs under visible irradiation [38].

It should be borne in mind that when a semiconductor is irradiated, those photoelectrons promoted to the conduction band could reduce certain metals on its surface. The photo-reduction of superficial Fe(III) species is a parallel reaction to the photocatalysis with iron oxides [39]. This photo-reduction may lead to the detachment of the iron species that, once in solution could produce $^{\bullet}$OH. However, no iron species were detected in the solution after irradiation as the photo-dissolution of the goethite is low [40]. Moreover, in Sn-substituted goethites, Sn(IV) is not easily photo-reduced (e.g. the reduction potential for the free species is much lower than that one for iron: $E^0_{Sn(IV)/Sn(II)} = 0.15$ V and $E^0_{Fe(III)/Fe(II)} = 0.77$ V; vs. NHE). This could disregard the formation of Fe(II) by charge transfer with tin: Sn(II) + 2Fe(III) $\rightarrow$ Sn(IV) + 2Fe(II).

Hence, it is not evident the role of the Sn in the enhancement of the Fenton process. Tin could participate in the Fenton reaction by either, a direct or an indirect route. The direct pathway may involve the formation

ACCEPTED MANUSCRIPT

of ROS onto the Sn surface sites and/or the charge transfer between the tin and the iron centers. As Sn is at its higher oxidation state, it cannot be oxidised by Fe(III), O_2 nor H_2O_2. Moreover, as mentioned above, it is not photoreduced, for which the direct pathway is thermodynamically not possible. In the case of the indirect pathway, the presence of tin could affect the iron speciation, as the balance of the Fe(II)/Fe(III) is important for the Fenton process [41]. The Sn(IV) forms an intermediate with the H_2O_2, named *tin hydroperoxo* (SnOOH) [42, 43], which could interact with a neighbour Fe(III), providing another pathway for the reduction of Fe(III) at expense of the H_2O_2 decomposition. This decomposition onto the goethites surface lead to the formation of ROS, mainly $^{\bullet}O_2H$ and $^{\bullet}OH$ [22]. The presence of these radicals was demonstrated by the addition of tert-butyl alcohol (TBA) as oxidative radicals scavenger (Fig. S5).

To summarise, the noticeable increase in the decolourisation yield under irradiation for all the samples could be understood as the higher ROS production by contribution of the following aspects: (i) the increase of hydroxyl surface species, as suggested by the correlation between the decolourisation yield and the amount of OSD, and (ii) the increase in the Fe(II)/Fe(III) ratio promoted simultaneously by the light and by the superficial SnOOH intermediate.

4.1. Proposed mechanism for MO decolourisation

In agreement with the proposed mechanism for heterogeneous Fenton, the initial steps for H_2O_2 decomposition in darkness onto the pure goethite sur-

Accepted Manuscript

ACCEPTED MANUSCRIPT

face can be described as follows. Firstly, the H_2O_2 complexates the goethite surface (≡Fe(III)-OH). Then, an electron transfer from ligand-to-metal produces a transitional state which is deactivated through the dissociation of the peroxide molecule and the reduction of iron (Eqs. 4 and 5). Finally, the superficial ≡Fe(II) species catalyses the generation of the hydroxyl radical ($^{\bullet}$OH) with the regeneration of the surface ≡Fe(III)-OH (Eq. 7) [44]:

$$\equiv Fe(III)\text{-}OH + H_2O_2 \rightleftharpoons (H_2O_2)_{ads} \tag{4}$$

$$(H_2O_2)_{ads} \rightleftharpoons \equiv Fe(III)\text{-}OOH + H_2O \tag{5}$$

$$\equiv Fe(II)\text{-}OOH \rightleftharpoons \equiv Fe(II) + {}^{\bullet}O_2H \tag{6}$$

$$\equiv Fe(II) + H_2O_2 \rightarrow \equiv Fe(III)\text{-}OH + {}^{\bullet}OH \tag{7}$$

Where $(H_2O_2)_{ads}$ refers to H_2O_2 adsorbed in the catalyst surface. Tin affects the cyclic reactions (Eqs. 4 to 6) by increasing the Fe(II)/Fe(III) ratio. As exposed before, Sn(IV) assists the Fe(III) reduction through the formation of the SnOOH intermediate. This proposed species could interact with a neighbour Fe(III) according to Eq. 8, followed by the formation of superficial Fe(II) species as indicated in Eq. 6:

$$\begin{aligned} \equiv Fe(III)\text{-}OH + \equiv Sn(IV)\text{-}OOH \rightleftharpoons \\ \equiv Fe(III)\text{-}OOH + \equiv Sn(IV)\text{-}OH \end{aligned} \tag{8}$$

The Fenton process assisted by light involves the photo-reduction of superficial Fe(III), increasing the presence of Fe(II) on the surface and gener-

ACCEPTED MANUSCRIPT

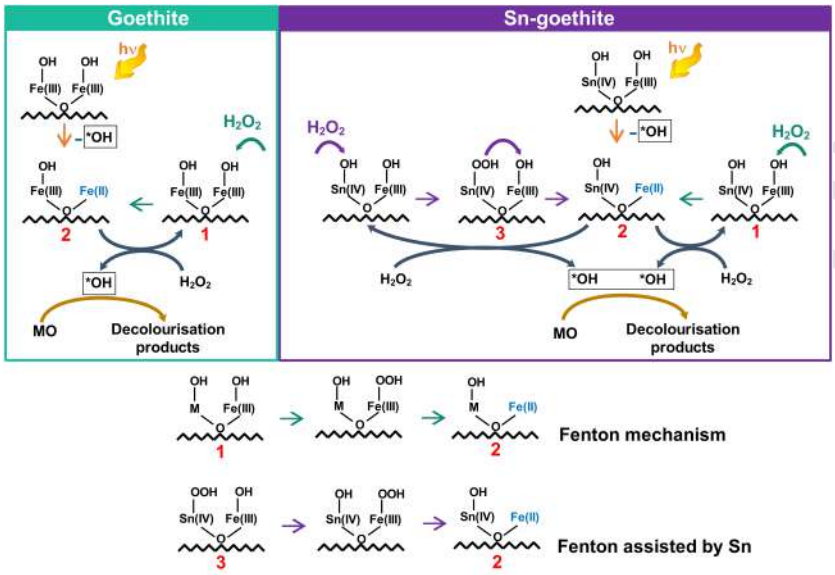

Figure 6: Proposed mechanism for the heterogeneous photo-Fenton process of MO in the presence of pure and tin substituted goethites.

ating more $^{\bullet}$OH, as shown in Eq. 9.

$$\equiv Fe(III)\text{-}OH + h\nu \rightarrow \equiv Fe(II) + {}^{\bullet}OH \tag{9}$$

The mechanism proposed in Eq. 4 to 9 for the reaction of Sn-substituted goethites in comparison to pure goethite is depicted in Fig. 6.

Since these reactions depend on the initial OH content, higher amounts of OSD enhance the H_2O_2 decomposition and, hence the MO decolourisation. With tin incorporation, the OSD reached a maximum for sample GSn2.1. The proposed mechanism suggests that tin participates in an indirect way in the MO decolourisation.

ACCEPTED MANUSCRIPT

5. Conclusions and perspectives

Tin-containing goethites showed an enhancement in the performance towards the MO decolourisation both via Fenton and photo-Fenton processes when compared to the pure sample. This catalytic improvement was attributed to changes in the OSD and the formation of an intermediate between the Sn and the H_2O_2 (SnOOH) which favours the decolourisation via the formation of Fe(II). The latter is a novel mechanism that involves the Sn in an indirect pathway, and no analogous was reported in Fenton and/or photo-Fenton processes.

However exploratory, this work offers new insights about the performance of this remarkable catalyst for the heterogeneous photo-Fenton process. Intermediate Sn substitutions should be explored in order to obtain the highest OSD. Moreover, the addition of a third metal that participates in the electron transfer (e.g. Cu, Mn or Co) may boost the generation of Fe(II). The promising results obtained in this work allow to design new and more efficient photo-catalysts for the decolourisation of dyes in natural samples.

Acknowledgements

This research was supported by grants PICT 2008, N°0780 from MINCyT (Argentina), PIP 11220170100289CO and UBACyT 20020170200298BA. D.O. and K.M.F. acknowledge CONICET for their postdoctoral fellowships. S.A.B is a member of CONICET.

References

Accepted Manuscript

ACCEPTED MANUSCRIPT

[1] V. Katheresan, J. Kansedo, S. Y. Lau, Efficiency of various recent wastewater dye removal methods: A review, Journal of Environmental Chemical Engineering 6 (2018) 4676–4697.

[2] J. J. Pignatello, E. Oliveros, A. MacKay, Advanced oxidation processes for organic contaminant destruction based on the fenton reaction and related chemistry, Critical Reviews in Environmental Science and Technology 36 (2006) 1–84.

[3] N. Wang, T. Zheng, G. Zhang, P. Wang, A review on Fenton-like processes for organic wastewater treatment, Journal of Environmental Chemical Engineering 4 (2016) 762–787.

[4] S. Rahim Pouran, A. R. Abdul Aziz, W. M. A. Wan Daud, Review on the main advances in photo-Fenton oxidation system for recalcitrant wastewaters, Journal of Industrial and Engineering Chemistry 21 (2015) 53–69.

[5] Q. Wu, H. Wang, C. Yi, Preparation of photo-Fenton heterogeneous catalyst (Fe-TS-1 zeolite) and its application in typical azo dye decoloration, Journal of Photochemistry and Photobiology A: Chemistry 356 (2018) 138–149.

[6] V. R. Elías, P. A. Ochoa Rodriguez, E. G. Vaschetto, G. A. Pecchi, C. Huck-Iriart, S. G. Casuscelli, G. A. Eimer, Tailoring the stability and photo-Fenton activity of Fe-modified nanostructured silicates by tuning the metal speciation from different synthesis conditions, Molecular Catalysis (2018) 1–13.

Accepted Manuscript

ACCEPTED MANUSCRIPT

[7] W. Shuai, C. Gu, G. Fang, D. Zhou, J. Gao, Effects of iron (hydr)oxides on the degradation of diethyl phthalate ester in heterogeneous (photo)-Fenton reactions, Journal of Environmental Sciences (China) (2018) 2–10.

[8] S. O. Ganiyu, M. Zhou, C. A. Martínez-Huitle, Heterogeneous electro-Fenton and photoelectro-Fenton processes: A critical review of fundamental principles and application for water/wastewater treatment, Applied Catalysis B: Environmental 235 (2018) 103–129.

[9] R. M. Cornell, U. Schwertmann, The iron oxides: structure, properties, reactions, occurrences and uses, 2003.

[10] a. Manceau, M. Schlegel, M. Musso, V. Sole, C. Gauthier, P. Petit, F. Trolard, Crystal chemistry of trace elements in natural and synthetic goethite, Geochimica et Cosmochimica Acta 64 (2000) 3643–3661.

[11] E. E. Sileo, L. García Rodenas, C. O. Paiva-Santos, P. W. Stephens, P. J. Morando, M. a. Blesa, Correlation of reactivity with structural factors in a series of Fe(II) substituted cobalt ferrites, Journal of Solid State Chemistry 179 (2006) 2237–2244.

[12] E. E. Sileo, A. Y. Ramos, G. E. Magaz, M. a. Blesa, Long-range vs. short-range ordering in synthetic Cr-substituted goethites, Geochimica et Cosmochimica Acta 68 (2004) 3053–3063.

[13] A. E. Tufo, M. dos Santos Afonso, E. E. Sileo, Arsenic adsorption onto aluminium-substituted goethite, Environmental Chemistry (2016) A–K.

Accepted Manuscript

ACCEPTED MANUSCRIPT

[14] M. Alvarez, a.E. Tufo, C. Zenobi, C. Ramos, E. Sileo, Chemical, structural and hyperfine characterization of goethites with simultaneous incorporation of manganese, cobalt and aluminum ions, Chemical Geology 414 (2015) 16–27.

[15] K. Rout, A. Dash, M. Mohapatra, S. Anand, Manganese doped goethite: Structural, optical and adsorption properties, Journal of Environmental Chemical Engineering 2 (2014) 434–443.

[16] H. Liu, T. Chen, R. L. Frost, An overview of the role of goethite surfaces in the environment., Chemosphere 103 (2014) 1–11.

[17] A. Gajović, A. M. Silva, R. A. Segundo, S. Šturm, B. Jančar, M. Čeh, Tailoring the phase composition and morphology of Bi-doped goethite-hematite nanostructures and their catalytic activity in the degradation of an actual pesticide using a photo-Fenton-like process, Applied Catalysis B: Environmental 103 (2011) 351–361.

[18] M. Alvarez, E. E. Sileo, E. H. Rueda, Structure and reactivity of synthetic Co-substituted goethites, American Mineralogist 93 (2008) 584–590.

[19] L. Hurtado, R. Romero, A. Mendoza, S. Brewer, K. Donkor, R. M. Gómez-Espinosa, R. Natividad, Paracetamol mineralization by Photo Fenton process catalyzed by a Cu/Fe-PILC under circumneutral pH conditions, Journal of Photochemistry and Photobiology A: Chemistry 373 (2019) 162–170.

ACCEPTED MANUSCRIPT

[20] M. C. Pereira, L. C. A. Oliveira, E. Murad, Iron oxide catalysts: Fenton and Fentonlike reactions a review, Clay Minerals 47 (2012) 285–302.

[21] Y. Wang, Y. Gao, L. Chen, H. Zhang, Goethite as an efficient heterogeneous Fenton catalyst for the degradation of methyl orange, Catalysis Today 252 (2015) 107–112.

[22] S. Rahim Pouran, A. A. Abdul Raman, W. M. A. Wan Daud, Review on the application of modified iron oxides as heterogeneous catalysts in Fenton reactions, Journal of Cleaner Production 64 (2014) 24–35.

[23] J. Xu, Y. Li, B. Yuan, C. Shen, M. Fu, H. Cui, W. Sun, Large scale preparation of Cu-doped α-FeOOH nanoflowers and their photo-Fenton-like catalytic degradation of diclofenac sodium, Chemical Engineering Journal 291 (2016) 174–183.

[24] B. Yuan, X. Li, K. Li, W. Chen, Degradation of dimethyl phthalate (DMP) in aqueous solution by UV/Si-FeOOH/H2O2, Colloids and Surfaces A: Physicochemical and Engineering Aspects 379 (2011) 157–162.

[25] A. L. Larralde, A. E. Tufo, P. J. Morando, E. E. Sileo, Enhanced As (V) Adsorption Properties in Sn-Substituted Goethites - Changes in Chemical Reactivity and Surface Characteristics, International Journal of Innovative Research in Engineering & Management (IJIREM) 2 (2015) 63–70.

[26] A. Larralde, C. Ramos, B. Arcondo, A. Tufo, C. Saragovi, E. Sileo, Structural properties and hyperfine characterization of Sn-substituted goethites, Materials Chemistry and Physics 133 (2012) 735–740.

Accepted Manuscript

ACCEPTED MANUSCRIPT

[27] F. J. Berry, Ö. Helgason, A. Bohórquez, J. F. Marco, J. McManus, E. A. Moore, S. Mørup, P. G. Wynn, Preparation and characterisation of tin-cloped α-FeOOH (goethite), Journal of Materials Chemistry 10 (2000) 1643–1648.

[28] X. Cui, J. Shi, Sn-based catalysts for Baeyer-Villiger oxidations by using hydrogen peroxide as oxidant, Science China Materials 59 (2016) 675–700.

[29] X. Meng, G. Qin, W. A. Goddard, S. Li, H. Pan, X. Wen, Y. Qin, L. Zuo, Theoretical understanding of enhanced photoelectrochemical catalytic activity of Sn-doped hematite: Anisotropic catalysis and effects of morin transition and Sn doping, Journal of Physical Chemistry C 117 (2013) 3779–3784.

[30] X. Li, Z. Si, Y. Lei, J. Tang, S. Wang, S. Su, S. Song, L. Zhao, H. Zhang, Direct hydrothermal synthesis of single-crystalline triangular Fe3O4 nanoprisms, 2010.

[31] L. Machala, R. Zboril, A. Gedanken, Amorphous iron(III) oxide - A review, Journal of Physical Chemistry B 111 (2007) 4003–4018.

[32] W. Li, L. Wang, F. Liu, X. Liang, X. Feng, W. Tan, L. Zheng, H. Yin, Effects of Al 3 + doping on the structure and properties of goethite and its adsorption behavior towards phosphate, Journal of Environmental Sciences (China) 45 (2015) 18–27.

[33] H. Liu, T. Chen, R. L. Frost, An overview of the role of goethite surfaces in the environment, Chemosphere 103 (2014) 1–11.

Accepted Manuscript

ACCEPTED MANUSCRIPT

[34] M. Mohapatra, S. K. Sahoo, S. Anand, R. P. Das, Removal of As (V) by Cu (II)-, Ni (II)-, or Co (II)-doped goethite samples, Journal of colloid and interface science 298 (2006) 6–12.

[35] Z. Cao, M. Qin, Y. Gu, B. Jia, P. Chen, X. Qu, Synthesis and characterization of Sn-doped hematite as visible light photocatalyst, Materials Research Bulletin 77 (2016) 41–47.

[36] Y. Nosaka, A. Y. Nosaka, Generation and Detection of Reactive Oxygen Species in Photocatalysis, Chemical Reviews 117 (2017) 11302–11336.

[37] D. L. Huang, P. L. Zhang, L. L. Qu, Q. Y. Chen, Dye-sensitized hematite compososite photocatalyst and its photocatalytic performance of aerobic annulation, Journal of Photochemistry and Photobiology A: Chemistry 360 (2018) 132–136.

[38] A. A. Jelle, M. Hmadeh, P. G. O'Brien, D. D. Perovic, G. A. Ozin, Photocatalytic Properties of All Four Polymorphs of Nanostructured Iron Oxyhydroxides, ChemNanoMat 2 (2016) 1047–1054.

[39] W. Feng, D. Nansheng, Photochemistry of hydrolytic iron (III) species and photoinduced degradation of organic compounds. A minireview, Chemosphere 41 (2000) 1137–1147.

[40] S. O. Pehkonen, R. Siefert, Y. Erel, S. Webb, M. R. Hoffmann, Photoreduction of Iron Oxyhydroxides in the Presence of Important Atmospheric Organic Compounds, Environmental Science and Technology 27 (1993) 2056–2062.

Accepted Manuscript

ACCEPTED MANUSCRIPT

[41] K. Rusevova, F. D. Kopinke, A. Georgi, Nano-sized magnetic iron oxides as catalysts for heterogeneous Fenton-like reactions-Influence of Fe(II)/Fe(III) ratio on catalytic performance, Journal of Hazardous Materials 241-242 (2012) 433–440.

[42] R. R. Sever, T. W. Root, Comparison of Epoxidation and BaeyerVilliger Reaction Pathways for Ti(IV)H2O2 and Sn(IV)H2O2, The Journal of Physical Chemistry B 107 (2003) 10521–10530.

[43] R. R. Sever, T. W. Root, Computational Study of Tin-Catalyzed BaeyerVilliger Reaction Pathways Using Hydrogen Peroxide as Oxidant, The Journal of Physical Chemistry B 107 (2003) 10848–10862.

[44] S. S. Lin, M. D. Gurol, Catalytic decomposition of hydrogen peroxide on iron oxide: Kinetics, mechanism, and implications, Environmental Science and Technology 32 (1998) 1417–1423.

Accepted Manuscript